AIAA 81-4294

Swirling Jets with and without Combustion

S. Fujii,* K. Eguchi,† and M. Gomi‡
National Aerospace Laboratory, Chofu, Tokyo, Japan

Strongly swirled, unconfined jets were quantified using a laser Doppler velocimeter measurement system with a unique, in-house single-particle processor under isothermal and combustion conditions. A drastic alteration of mean flow profiles was recognized as a result of combustion. Deviations of the swirl velocity from a solid-body rotation in the flame zone were probably due to unstabilizing effects caused by the viscous forces which outweighed the centrifugal forces. Turbulence levels were higher in the reacting flow with a scatter of the measured data than in the isothermal jet. It may be deduced that time-dependent variations of the density as well as the flame location, caused by interaction of chemical reaction/turbulence, produced the scattered data and hence the flame-generated turbulence. The experimental data indicate that the turbulence local equilibrium model may be accepted in the reacting strongly swirled jet.

Nomenclature

D	= outer diameter of burner exit (= 60 or 100 mm)
G_θ	$= \int_0^\infty \rho r^2 UW \mathrm{d}r$
G_x	$= \int_0^\infty \rho r(U^2 - W^2/2)\mathrm{d}r$
k	= turbulence kinetic energy, $k = (\overline{u^2} + \overline{v^2} + \overline{w^2})/2$
$k_{\max}$	= maximum of k at a measuring station
$r_{0.5}$	= half velocity radius
(r,θ,z)	= cylindrical coordinates with z downstream
S	= swirl number, $S = G_\theta/(G_x D/2)$
(V,W,U)	= radial, swirl, and axial mean velocity
(v,w,u)	= turbulence instantaneous velocity
(V_0,W_0,U_0)	= velocity scales, maximum of (V,W,U) at a measuring station
(V_{0m},W_{0m},U_{0m})	= maximum velocity at exit plane
$(\overline{v^2}, \overline{w^2}, \overline{u^2}, \overline{wv}$, etc.)	= turbulence velocity correlation
z_0	= virtual origin
α,β	= angle of traverse-bench rotation
ϕ_p	= equivalence ratio of propane/air mixture
ρ	= time-averaged density

Subscripts and Superscripts

1,2	= velocities associated with the laser position in Fig. 2

Introduction

EXPERIMENTAL observations of swirling flows have been made for a number of years. It appears that they can be roughly categorized by the following three different flow configurations. The experiment of vortex breakdowns[1,2] is considered the first group and may be usually approximated by an inviscid analysis.[3] The swirling isothermal flow belongs to the second cluster and has been approached primarily by means of a hot-wire anemometer.[4-7] The swirling flame may fall into the last group, which has particular relevance to furnace flows and burners.[8-10] The advent of a laser Doppler velocimeter (LDV) has had a significant impact on data acquisition in complex flows under the combustion environment. Advances in all aspects of swirling flow/flame research were extensively reviewed in the references.[11,12]

The present work deals with unconfined, swirling turbulent flow under both isothermal and combustion conditions. An LDV measurement system was employed to quantify the velocity characteristics of jets emerging from the swirl burner. The major objective of this paper is to present the flow data on swirl and to improve understanding of the relevant physical process that is still insufficient to allow a satisfactory turbulence model closure. Previous data reported in the open literature are less detailed than is necessary for the present purpose. They do not include measurements of the detailed profiles of mean flow and turbulence velocity correlation, particularly in regions of recirculation during combustion. The measurements described herein encompass the three velocity components of mean flow and turbulence velocity correlations. Emphasis is placed upon the comparison of fluid dynamic characteristics with and without combustion.

Test Facility, Flow Configuration, and Instrumentation

Test Setup

The test rig is shown in Fig. 1. For measurements with isothermal flow, compressed air by a centrifugal blower was supplied through a settling chamber to a swirl generator which consisted of a row of vanes. The outer and inner diameters of the annular section were 100/70 mm and 60/40 mm, respectively. For the single jet test, the outer annulus was blocked

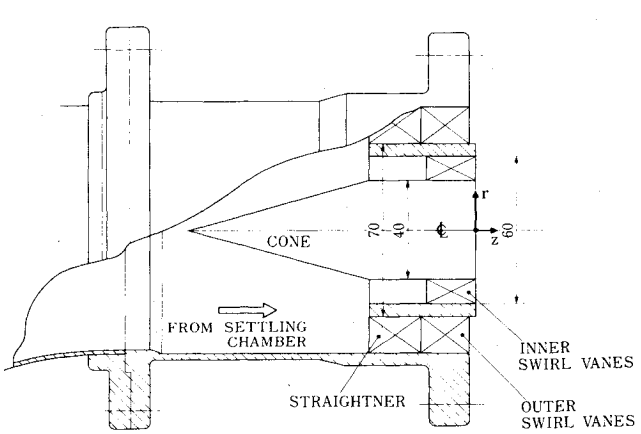

Fig. 1 Flow enclosure and swirl jet burner (units, mm).

Received Feb. 19, 1981.

*Head, Engine Noise Group.
†Senior Researcher, Aero-Engine Division. Member AIAA.
‡Research Engineer, Engine Noise Group.

Table 1 Flow arrangements

Flow description	Identification	Outer diameter, mm	Inner diameter, mm	Reynolds number	Swirl number,[b] S	Outer vane lead angle, deg	Inner value lead angle, deg
Isothermal single[a]	S_1	...	60	10^5	1.50	...	45
Isothermal single	S_2	...	60	10^5	0.69	...	30
Isothermal double	S_3	100	60	1.7×10^5	0.78	45	30
Reacting single[a]	C	...	60	10^5	0.90	...	45

[a] S_1 and C have the same vane angle. [b] Uncertainty of $S=\pm0.03$.

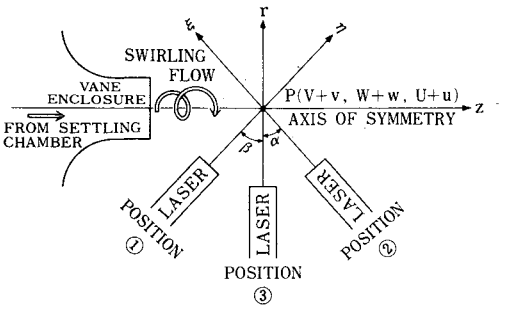

Fig. 2 Layout of the measurement by rotation of traverse bench.

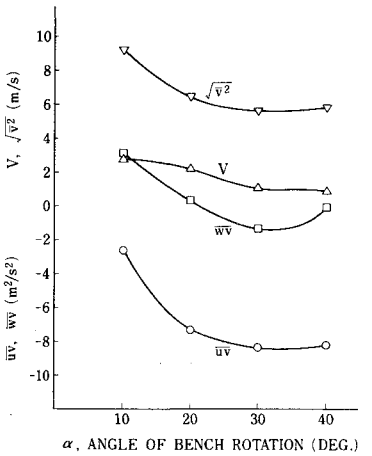

Fig. 3 Effect of rotation angles on the measured velocity.

off at the exit. A homogeneous propane/air mixture was used in the combustion flow testing. Propane and air were metered by the respective orifice and premixed before entering into the settling chamber. The flow was seeded with small concentrations of titanium dioxide particles for the LDV measurement. The rate of particles in a sensing volume was about 50/s.

The flow arrangements reported in this paper are summarized in Table 1. Three different configurations denoted as S_1, S_2, and S_3 were first tested under the isothermal conditions, and then one of them, S_1, was selected for further testing, C, under the combustion. The vane angle was varied to change the degree of rotation imparted to air. The Reynolds numbers indicated in the table were based on the burner diameter and isothermal flow properties. To characterize the helicity of the flow, the swirl number was calculated from the measured data for each configuration. Despite the same geometrical configuration, the difference in the swirl number of C from S_1 was attributed to a marked increase of axial thrust due to heat addition.

Flow traverses were performed in downstream regions covering $0.5\le z/D\le5.0$ except for the coaxial case, S_3, which ranged from $z/D=0.5$ to 3.0. The laser beam was moved at an interval of 2.0 mm in radial direction.

Instrument

The LDV and data acquisition system used are exactly the same as those in Ref. 13. It comprised a 15-mW HeNe laser (Spectra-Physics 124A) and a signal processor of tracker type (TSI-Kanomax 27-series) with a velocity offset device to avoid the directional ambiguity. The flow data processed were acquired through an in-house single-particle processor into a minicomputer. The processor was programmed to read only one velocity signal as a seeding particle passed in the sensing volume, so that reliability of the measurement data might be improved in the high turbulence flow. Further detailed information on the single-particle processor is given in Ref. 14.

Flow Determination

All optical instruments such as laser tube, lenses, and photomultiplier were placed on a traverse bench moving three dimensionally and rotating around its axis. To determine the velocity at a point of P that is fixed in space, Fig. 2, the forward-scattered light was rotated around the bench axis and stopped at three different positions with the focus kept upon the point. At each bench rotation, the beam was further rotated around the laser tube axis to determine other components of velocity on that plane. If the point of P had an instantaneous velocity defined as $(V+v, W+w, U+u)$ in the swirling jet, its time-averaged velocity components and correlations were determined by solving a set of simultaneous equations, such that

$$V\sin\alpha+U\cos\alpha=U_1 \tag{1}$$

$$-V\sin\beta+U\cos\beta=U_2 \tag{2}$$

$$\overline{v^2}\sin^2\alpha+2\overline{uv}\sin\alpha\cos\alpha+\overline{u^2}\cos^2\alpha=\overline{u_1^2} \tag{3}$$

$$\overline{v^2}\sin^2\beta-2\overline{uv}\sin\beta\cos\beta+\overline{u^2}\cos^2\beta=\overline{u_2^2} \tag{4}$$

$$\overline{vw}\sin\alpha+\overline{uw}\cos\alpha=\overline{u_1w_1} \tag{5}$$

$$-\overline{vw}\sin\beta+\overline{uw}\cos\beta=\overline{u_2w_2} \tag{6}$$

together with the simple relationship of

$$W=W_1=W_2 \quad \text{and} \quad \overline{w^2}=\overline{w_1^2}=\overline{w_2^2} \tag{7}$$

Experimental Uncertainty

During the combustion tests, ample spacing was needed between the jet flame and the optical instruments to prevent heat damage. To this end, a focal length of 583 mm was chosen in all measurements, which resulted in a sensing volume of elliptic spatial resolution with a principal axis of 0.3 and 7.7 mm. A thoughtful comparison of the LDV, hot-wire, and pitot tube, made on the nonswirling jet, showed that the LDV gave rise to a 5-6% smaller mean velocity than other probes only in steep velocity-gradient regions.

An error introduced in rotating the bench axis was estimated next. With $\alpha=\beta$ postulated, solution of Eqs. (1-6) depends on terms of $1/\sin2\alpha$, so that α should be as close as possible to 45 deg in order to minimize the error associated with rotation. Effects of the angle of rotation on the measured values, made on a fixed point of the isothermal swirling jet, were illustrated in Fig. 3. As the data tended to their finite value beyond $\alpha=30$ deg, the measurements

reported herein were mostly performed with $\alpha = 40$ deg. The traversing mechanism allowed positioning to within ± 0.05 mm and ± 0.05 deg at any desired angular position. The jet was substantially axisymmetric in entire downstream stations not extremely close to the burner exit. The measurement errors in this experiment were then evaluated as follows: uncertainty of U, $W = \pm 1.0$ m/s, $V = \pm 2.0$ m/s; uncertainty of $\overline{u^2}$, $\overline{w^2}$, $\overline{uw} = \pm 1\ \mathrm{m^2/s^2}$, $\overline{v^2}$, $\overline{uv}$, $\overline{wv}$, $\overline{k^2} = \pm 2\ \mathrm{m^2/s^2}$.

Experimental Observations and Discussion

Mean Flow Data

Axial velocity distributions with observations parallel to the axis of symmetry are compared in Fig. 4. It is noted that the coaxial, S_3, and the single jet, S_1, had almost the same axial extent of recirculation bubble despite their difference in the swirl number. The profile in combustion is very distinct from the isothermal ones. In comparing S_1 and C cases, which had the same vane angle, the axial length of the bubble was diminished and the point of maximum recirculation strength necessary for the flame stabilization shifted further downstream, due to the heat release. These results greatly differ from the LDV observations of the weakly swirling jets by Chigier and Dovrak.[9]

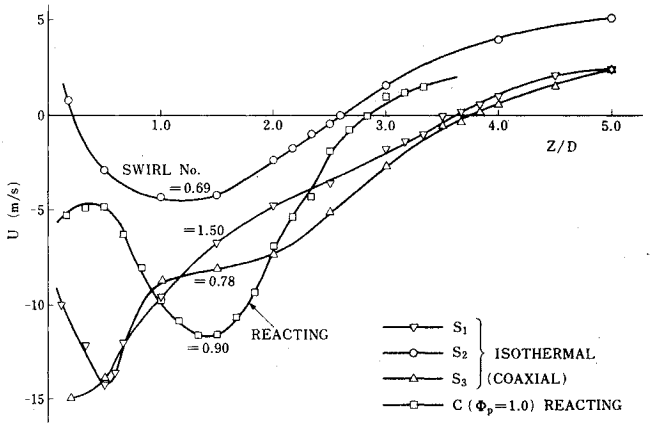

Fig. 4 Axial velocity distributions along the axis of symmetry.

Figure 5 shows the radial spread of swirling jets with distance downstream in comparison with the result of Pratte and Keffer,[5] who showed that the position of virtual jet source was independent of the swirl numbers when they were less than 0.35. As the present data revealed, however, the virtual origin, z_0, no longer coincided as the swirl number became stronger and/or combustion commenced. It is notable that the lesser spread of axial velocity was recognized in the reacting flow.

The streamwise variation of maxima of the mean velocity components is illustrated in Fig. 6. The decay rate followed a trend towards the similarity of the weakly swirled jets in regions of $(z - z_0)/D \geq 4$, where the isothermal jets were considered to be comparatively developed.

Typical radial-distributions of the mean flow were selected for the cases of S_1 and C at $z/D = 1.0$ and compared in Figs. 7a and 7b. It is first noticed that the swirl component was significantly distorted around the flame stabilized zone with sharp axial-velocity gradients, whereas a solid-body rotation was maintained in the isothermal flow. The stability of reacting, stratified flows depends on the modified Richardson number,[15] defined by $R^* = (1/\rho)(\partial\rho/\partial r)(W^2/r)/(\partial U/\partial r)^2$, indicative of a ratio of centrifugal to shear forces. Since the Richardson number became very low in the flame stabilized zone, where values of $(\partial U/\partial r)^2$ were quite large, it may be suggested that the distorted profile of W was probably attributed to an unstable effect produced by shear forces which outweighed centrifugal forces.

One more discrepancy is that the radial and swirl velocity were of the same order of magnitude outside the hot bubble, which implies that the outward movement of the reacting flow was predominant. Furthermore, the negligible smallness of V measured in the hot recirculation was suggestive of an important cue in the flame stabilizing effect.

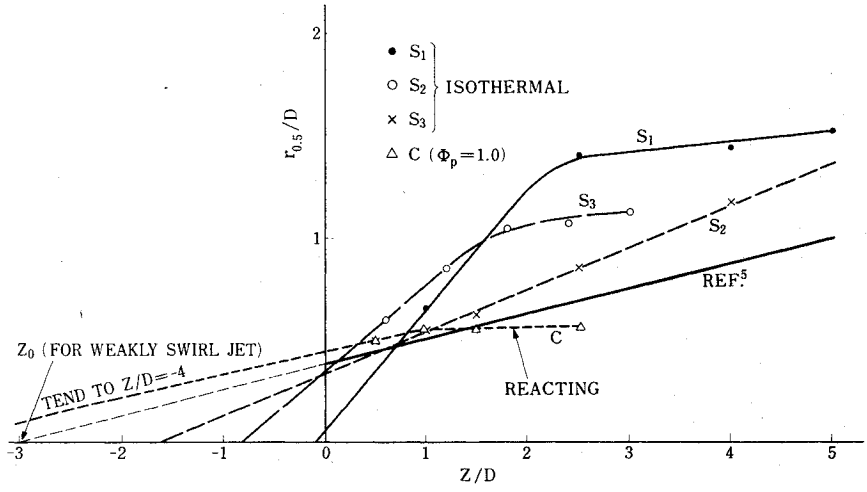

Fig. 5 Radial spread of the swirling jets and their virtual origins.

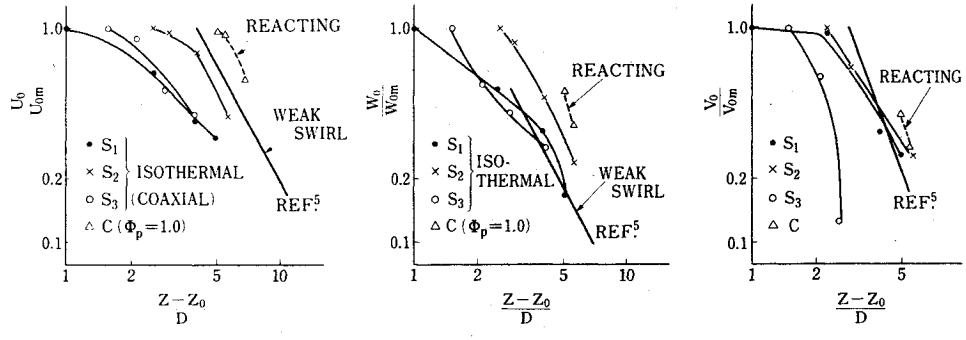

Fig. 6 Decay of mean velocity scales.

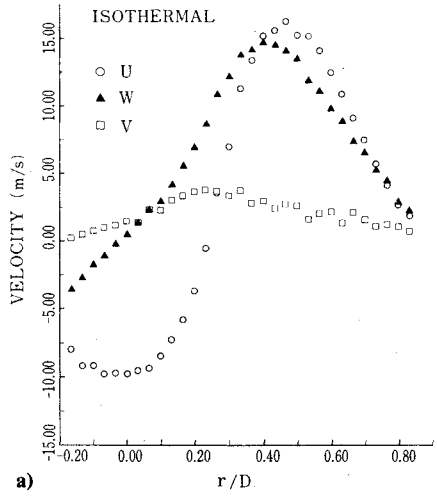

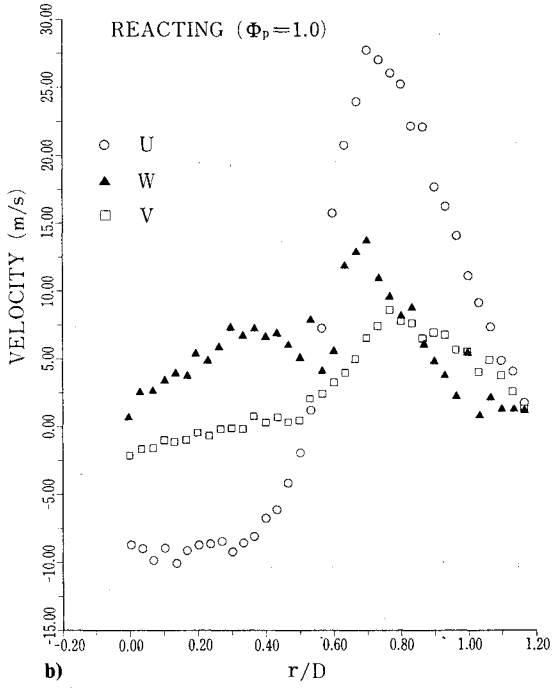

Fig. 7 Radial distributions of the mean flow at $z/D=1.0$: a) isothermal, S_1; b) reacting ($\phi_p=1.0$), C.

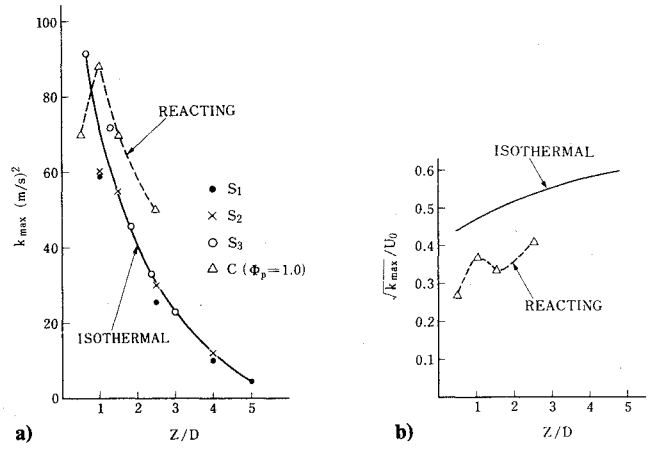

Fig. 8 Streamwise variations of turbulence kinetic energy: a) k_{max}; b) normalized by the local maximum velocity.

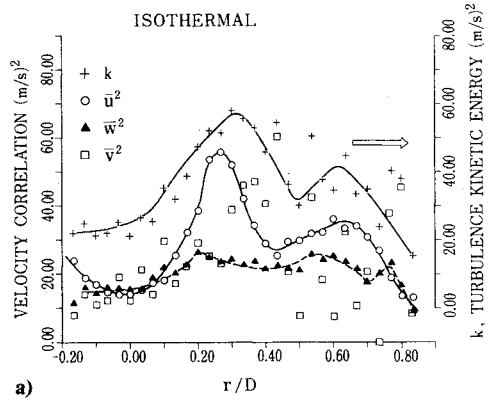

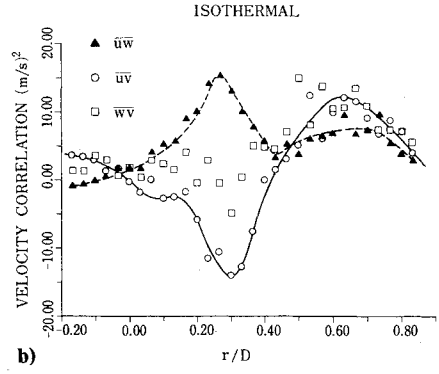

Fig. 9 Isothermal turbulence properties for S_1 at $z/D=1.0$: a) normal; b) shear.

Chigier[8] concluded that chemical reaction and temperature changes caused only minor perturbation to the main flowfield in the swirling flame with swirl numbers less than 0.3. The case is different with the strongly swirling flow discussed in this paper.

Turbulence Velocity Correlation

Turbulence quantities of the swirling jet under isothermal and combustion conditions are compared in Figs. 8-10. The streamwise variations of maximum turbulence kinetic energy are indicated in Fig. 8. Figure 8a shows that an increase in turbulence level was observed beyond the point of $z/D=1$ in combustion. In addition, the same data were nondimensionalized by a maximum of axial velocities at each measuring station and plotted in Fig. 8b, which showed in turn an apparent suppression of turbulence kinetic energy as a consequence of combustion.

The increase of turbulence level due to combustion was already reported for the nonswirling[16] and swirling jet[9] in terms of burner exit condition; on the other hand, Glass and Bilger[17] reported a suppression of $\overline{u^2}/U_0$ where U_0 represents the local maximum. It is also noted that a decrease in turbulence level was observed only near the burner exit where the reacting flow was not yet established.[9] These results are in qualitative agreement with the present data.

Selected results for S_1 and C at $z/D=1.0$ are compared in Figs. 9 and 10. Figure 9a shows that a double peak of $\overline{u^2}$ and k was produced in regions with high gradients of the mean axial velocity without combustion. If combustion commenced, the peaks were much pronounced at $r/D=0.56$, around which the flame was established (Fig. 10a). Another difference in both flows is that the measured data of $\overline{w^2}$ were considerably scattered in the entire region of the combustion flow. With regard to the normal stresses plotted in Figs. 9a and 10a, the isotropic turbulence was maintained only near the axis of symmetry in the isothermal flow and deviations from the isotropy were significant in other regions and particularly in the reacting flow.

Other turbulence velocity correlations are plotted in Figs. 9b and 10b. Rather dispersive distributions of uw and wv were

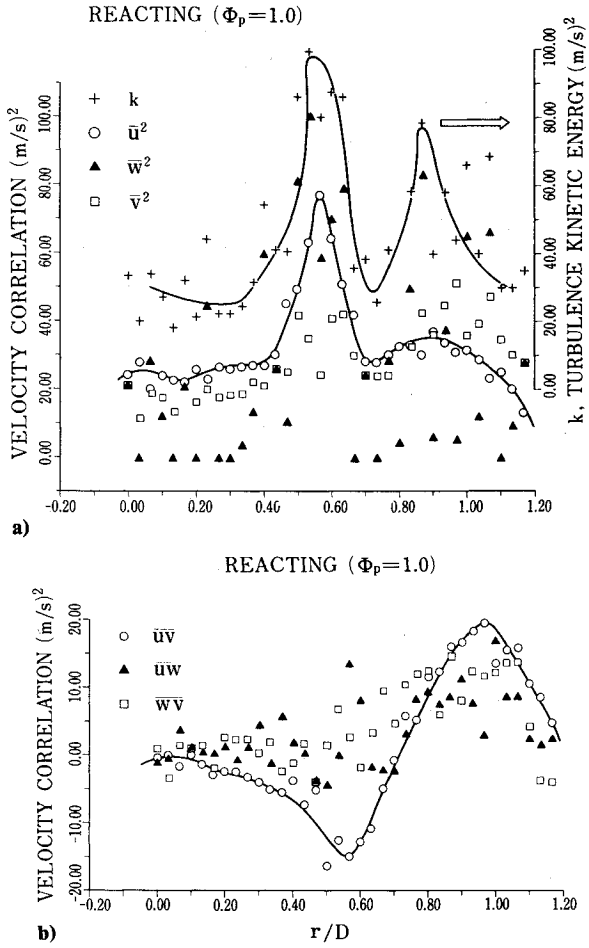

Fig. 10 Reacting turbulence properties for C at $z/D = 1.0$: a) normal; b) shear.

also found in the reacting flow data, which might be attributed to the scattered data of $\overline{w^2}$. It appears that interaction of turbulence/chemical reaction caused the time-dependent variations of the density as well as the flame position, which resulted in the scatter of the measured flow data. This phenomenon may be what is called the flame or combustion generated turbulence. In addition to this, it must be recalled that the turbulence could be generated by an increase of $\partial U/\partial r$ observed in the combustion data and destroyed or suppressed by the dilatation effect[18,19] due to heat release.

Another interesting feature is that the products of $-\overline{uv}\partial U/\partial r$, characteristic of the turbulence energy production in the nonswirling boundary layer, were always positive in the present data with and without combustion, and, further, that the positions where uv and $\partial U/\partial r$ approach zero occurred at the same point. Since the same reasoning can be applied to the products of $-\overline{wv}\, r(\partial W/r/\partial r)$, the familiar Prandtl model[20] such as $-\overline{uv} \propto [(\partial U/\partial r)^2 + (r\partial W/r/\partial r)^2]$ under the boundary layer approximation, may be acceptable in the complex, reacting flow. A double peak of the distributions of $\overline{uw}$ was observed in the regions with high gradients of $\partial U/\partial r$ and $r(\partial W/r/\partial r)$, which again shows a strong dependence of the Reynolds stresses on the local strain of mean flows.

Summary

The net results of the experimental aspects for the strongly swirled jets are summarized in the following.

1) Virtual origins of the radial spread curves did not coincide as the swirl number became strong and/or combustion commenced.

2) The reacting jet had a pronounced outward movement outside the recirculation, with the radial motion suppressed in the hot bubble, which significantly contrasted with the gradual increase and decrease of the radial velocity detected in the isothermal jet.

3) Deviations from a solid-body distribution of the swirl velocity in the flame zone were probably attributed to the strong viscous forces which outweighed the centrifugal forces, as can be explained by the modified Richardson number.

4) The turbulence levels were increased as a consequence of combustion, with an attendant scatter of the measured turbulent velocities. It is tentatively concluded that the fluctuations of the density as well as the flame location, caused by interaction of combustion/turbulence, might produce the scattered data which in turn appeared as the flame generated turbulence.

5) Relationships obtained between the turbulence velocity correlations and the mean flow gradients showed that the turbulence local equilibrium model, depending on the local strain of mean flows, could be acceptable in the complex swirling jets with and without combustion.

References

[1] Harvey, J.K., "Some Observations of the Vortex Breakdown Phenomena," *Journal of Fluid Mechanics*, Vol. 14, Dec. 1962, pp. 585-592.

[2] Sarpkaya, T., "Vortex Breakdown in Swirling Conical Flows," *AIAA Journal*, Vol. 9, Sept. 1971, pp. 1792-1799.

[3] Bossel, H.H., "Vortex Breakdown Flowfield," *Physics of Fluids*, Vol. 12, March 1969, pp. 498-508.

[4] Chigier, N.A. and Chervinsky, A., "Experimental Investigation of Swirling Vortex Motion in Jets," *Journal of Applied Mechanics, Transactions of ASME*, Vol. 34, June 1967, pp. 443-451.

[5] Pratte, B.D. and Keffer, J.F., "The Swirling Turbulent Jet," *Journal of Basic Engineering, Transactions of ASME*, Vol. 94, Dec. 1972, pp. 739-748.

[6] Ribeiro, M.M. and Whitelaw, J.H., "Coaxial Jets with and without Swirl," *Journal of Fluid Mechanics*, Vol. 96, 1980, pp. 769-795.

[7] Habib, M.A. and Whitelaw, J.H., "Velocity Characteristics of Confined Coaxial Jets with and without Swirl," *Journal of Fluids Engineering, Transactions of ASME*, Vol. 102, March 1980, pp. 47-53.

[8] Chigier, N.A., "Gas Dynamics of Swirling Flow in Combustion Systems," *Astronautica Acta*, Vol. 17, 1972, pp. 387-395.

[9] Chigier, N.A. and Dovrak, K., "Laser Anemometer Measurements in Flames with Swirl," *15th Symposium (International) on Combustion*, The Combustion Institute, 1975, pp. 573-585.

[10] Baker, R.J., Hutchinson, P., Khalil, E.E., and Whitelaw, J.H., "Measurements of Three Velocity Components in a Model Furnace with and without Combustion," *15th Symposium (International) on Combustion*, The Combustion Institute, 1975, pp. 553-559.

[11] Syred, N. and Beer, J.M., "Combustion in Swirling Flows: A Review," *Combustion and Flame*, Vol. 23, Oct. 1974, pp. 143-201.

[12] Lilley, D.G., "Swirl Flows in Combustion: A Review," *AIAA Journal*, Vol. 15, Aug. 1977, pp. 1063-1078.

[13] Fujii, S., Gomi, M., and Eguchi, K., "Cold Flow Tests of a Bluff-Body Flame Stabilizer," *Journal of Fluids Engineering, Transactions of ASME*, Vol. 100, Sept. 1978, pp. 323-332.

[14] Gomi, M., Kidawara, S., and Fujii, S., "A Method of Laser Velocimeter Data Processing," National Aerospace Laboratory Technical Report TR-521, Jan. 1978 (in Japanese with English summary).

[15] Beer, J.M., Chigier, N.A., Davies, T.W., and Bassindale, K., "Laminarization of Turbulent Flames in Rotating Environments," *Combustion and Flame*, Vol. 16, Feb. 1971, pp. 39-45.

[16] Starner, S.H. and Bilger, R.W., "LDA Measurements in a Turbulent Diffusion Flame with Axial Pressure Gradient," *Combustion Science and Technology*, Vol. 21, Mar. 1980, pp. 259-276.

[17] Glass, M. and Bilger, R.W., "The Turbulent Jet Diffusion Flame in a Co-flowing Stream—Some Velocity Measurements," *Combustion Science and Technology*, Vol. 18, Sept. 1978, pp. 165-177.

[18] Bray, K.N.C. and Libby, P.A., "Interaction Effects in Turbulent Premixed Flames," *Physics of Fluids*, Vol. 19, Nov. 1976, pp. 1687-1701.

[19] Fujii, S. and Eguchi, K., "A Comparison of Cold and Reacting Flows Around a Bluff-Body Flame Stabilizer, *Journal of Fluids Engineering, Transactions of ASME*, Vol. 103, June 1981, pp. 328-334.

[20] Lilley, D.G., "Nonisotropic Turbulence in Swirling Flows," *Acta Astronautica*, Vol. 3, Nov.-Dec. 1976, pp. 919-933.